Towards Dynamic Task/Posture Control of a 4DOF Humanoid Robotic Arm

Omar T. Abdelaziz[1], Shady A. Maged[2], Mohammed I. Awad[3]
Mechatronics Engineering Department, Faculty of Engineering, Ain Shams University, Cairo, Egypt
Emails: [1]omar_t40@hotmail.com, [2]shady.maged@eng.asu.edu.eg, [3]mohammed.awad@eng.asu.edu.eg

***Abstract*—A comparison between two control schemes of a humanoid robot arm is considered, facilitating the development of humanoids that have human-like movements and safe to operate in the vicinity of humans. This paper describes modeling and simulation of a 4 degree of freedom (DOF) INMOOV humanoid robotic arm using MATLAB/Simmechanics toolbox. The proportional derivative (PD) control and sliding mode control (SMC) based on the operational space formulation of task/posture control is considered. The comparison between the two controller approaches in respect to accuracy, natural movement and time response is also presented, showing the effectiveness of the SMC over the PD controller.**

***Index Terms*—humanoid robot, sliding mode control, proportional derivative control, biologically inspired arm control.**

I. Introduction

All through the history of mankind, copying from nature has helped in getting optimum design and better performances through designs that imitate the human body structure and function. Humanoid robotics has the potential to be used in social robotics as it has similar human shape. This approach is general and versatile as it can interact with humans in many different environments and situations to perform many tasks. Humanoid robots also should have similar geometry, kinematics, sensing capabilities and behavior to humans [1]. This has enabled these robots to be developed as general-purpose platforms, in the entertainment industry, defense industry and to study human behavior [2][3].

The history of human form imitation began long ago in the 13th century by Al-Jazari and in the 15th century by Leonardo da Vinci, both designed humanoid automation [4]. The first modern humanoid was WABOT-1 which was developed at Waseda University in Japan as mentioned in [1]. Many developments were made to the humanoid robotics field by many researchers as in [5] -[9].

For most applications of the humanoid robot, both kinematic and dynamic modeling is needed, which is introduced by a lot of researchers as in [10] - [13].

Human-Like reaching motion has a vital role in the human robot movement control and interaction, for this reason biologically inspired control methods were developed [14]. To implement this type of control a dynamically based force control method is a must. For this reason, Spiers et al. [15] presented a biologically inspired controller, using a redundant degree of freedom to separate the control into task and posture control. This separation is based on the work of Khatib [16] on the operational space controller and the inertial coupled pseudo inverse.

The Proportional Derivative is one of the most versatile controllers. It was implemented on the operational space controller in [15] on two DOF, shoulder and elbow flexion of BERT robot arm.

Furthermore, sliding mode controller (SMC) is one of the attractive types of robust controller schemes as sliding surface is used to force the error of the task variables into zero [17]. Qin et al. [18] proposed an adaptive back stepping sliding mode for hybrid serial parallel humanoid robot. Moreover, sliding mode control with the gravity compensation was implemented in [19] on the NTU humanoid robot arm. While, the sliding mode control was applied also on the task/posture control in [20]

In this manuscript, The PD controller is implemented on the task control using feedback linearization. Also, it is used to optimize the effort function in the posture control. Furthermore, the sliding mode controller is also implemented in this paper as a second controller. Both controllers are modeled and simulated on the 4 DOF INMOOV arm using MATLAB/Simulink. A comparative study between the two controllers on terms of accuracy, human-like movements and time response are considered.

This paper is organized as follows. Section II introduces the kinematic model of INMOOV arm. Section III presents the operational space controller. Section IV demonstrates the proportional derivative (PD) controller. The sliding mode controller (SMC) is presented in Section V. Simulation and discussion are shown in section VI and finally the concluding remarks are drawn in section VII

II. Kinematic Model Analysis

In this section, the forward kinematics using Denavit-Hartenberg (D-H) parameters of the INMOOV 4 DOF humanoid robotic arm will be presented with the aid of the PeterCorke/Robotics toolbox for MATLAB.

Consider the INMOOV humanoid robotic arm as shown in Fig. 1. It has a total of 10 degrees of freedom, 3

Manuscript received June 25, 2018; revised July 4, 2019.

© 2020 Int. J. Mech. Eng. Rob. Res

in the shoulder, 1 in the elbow, 1 for the wrist and 1 for each finger. Only 4-DoF, 3-DoF for the shoulder and 1-DoF for the elbow joints, are considered in this study.

From the coordinate system which is shown in Fig. 1, the D-H parameters of the arm model is derived using D-H convention as shown in Table I.

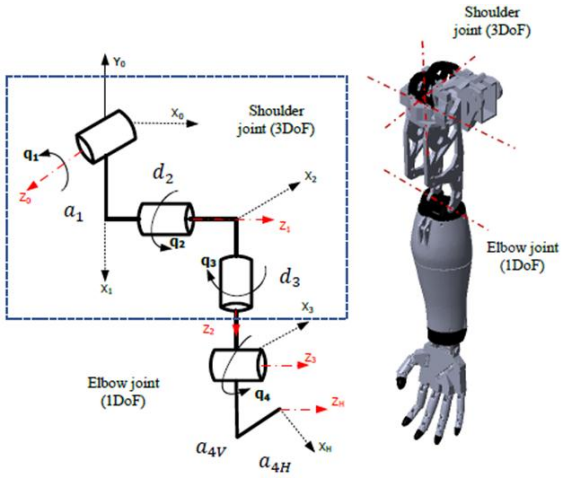

Figure 1. INMOOV robotic arm model

TABLE 1. D-H MODEL PARAMETERS

Joint	a_i	α_i	d_i	θ_i	Offset
1	a_1	$\pi/2$	0	q_1	$-\pi/2$
2	0	$\pi/2$	d_2	q_2	$\pi/2$
3	0	$-\pi/2$	d_3	q_3	0
H	a_4	0	0	q_4	O_4

Where $a_1 = 52.98\ mm$, $d_2 = 132.19\ mm$, $d_3 = 275.85\ mm$, $a_{4V} = 350\ mm$, $a_{4H} = 50\ mm$, $a_4 = \sqrt{a_{4V}^2 + a_{4H}^2}$, $O_4 = -\left(\frac{\pi}{2} - tan^{-1}\frac{a_{4H}}{a_{4V}}\right) = -81.87^{\circ}$

III. OPERATIONAL SPACE CONTROLLER

The operational space controller block diagram shown in fig. 2 is a force control method that is based on separating the robot dynamics into task space and null space according to the following:

$$\text{Total Torque} = \mathrm{T_t} + \mathrm{T_p} \tag{1}$$

T_t is the task control torque which is given a priority, while T_p the posture control torque is in the null space of the task control.

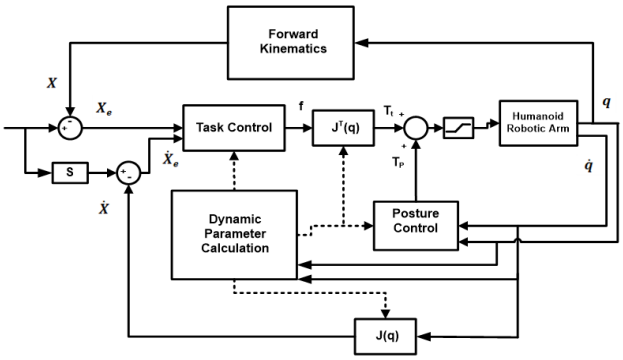

Figure 2.: Control block diagram

A. Task Control

To Control this robotic arm dynamically the following Lagrange equation is used:

$$T = M(q)\ddot{q} + C(q,\dot{q}) + G(q) \tag{2}$$

$M(q)$ is the inertial matrix, $C(q,\dot{q})$ is the Coriolis and Centrifugal matrix, and $G(q)$ is the gravitational matrix. These dynamic parameters where produced symbolically from the PeterCorke/Robotics toolbox for MATLAB according to robot kinematic and dynamic parameters.

The task control torque that drives the robot to the demand position is determined from eq. (2) by replacing T by T_t. The projection of the task variables from the joint-space to the Cartesian space using Jacobian pseudo inverse is given in [16].

$$J^{-T}(T_t) = J^{-T}\left(M(q)\ddot{q} + C(q,\dot{q}) + G(q)\right) \tag{3}$$

$$f = \Lambda(q)\ddot{X} + \mu(q,\dot{q}) + p(q) \tag{4}$$

where:

$$J^{-1} = M^{-1}J^{T}\Lambda \tag{5}$$
$$\Lambda = (JM^{-1}J^{T})^{-1} \tag{6}$$
$$\mu = J^{-T}C - \Lambda\dot{J}\dot{q} \tag{7}$$
$$p = J^{-T}G(q) \tag{8}$$

And f is the cartesian force vector.

Then, the task control torque is calculated from the force:

$$T_t = J^{T}f \tag{9}$$

B. Posture Controller

The posture control torque is concerned with the trajectory of the robotic arm to achieve natural human-like movement. An effort function was proposed based on the gravitational forces. The optimized effort function will ensure a human-like motion trajectory [15]. This effort function is calculated based on the following equation:

$$U = G(q)^{T}{K_a}^{-1}G(q) + K_L\sum_{i=1}^{n}\frac{1}{|q_i - q_{Li}|^{K_{Li}} + \delta_{Li}} \tag{10}$$

where q_{Li} are the joint limits and K_L , K_{Li} and δ_{Li} are positive scalar constants, i is the joint index. K_a is activation matrix which is a $4X4$ diagonal matrix as follows:

$$\begin{bmatrix} K_{a1} & 0 & 0 & 0 \\ 0 & K_{a2} & 0 & 0 \\ 0 & 0 & K_{a3} & 0 \\ 0 & 0 & 0 & K_{a4} \end{bmatrix}$$

where $K_{ai}, i = 1, \ldots n$ represents the effect of each link i on the effort function. The minimization of effort function using PD and SMC will be presented in the following sections.

© 2020 Int. J. Mech. Eng. Rob. Res

IV. Proportional Derivative Controller

This Section shows both the feedback linearization task control and PD optimization for the posture control

A. Feedback Linearization for Task Control

A modification is made to the task control by substituting the acceleration ($\ddot{X}$) in eq. (4) with f^* as follows:

$$f = \Lambda(q)f^* + \mu(q,\dot{q}) + p(q) \tag{11}$$

The feedback linearization is done as follows:

$$f^* = -K_x X_e - K_v \dot{X}_e \tag{12}$$

where K_x and K_v are positive scalar constants, $\dot{X}_e$ is the velocity position error and X_e is the position error vector calculated in the following equation:

$$X_e = X_d - X_a \tag{13}$$

where X_d is the demand position vector $[X_d\ Y_d\ Z_d]^T$ and X_a is the actual position vector $[X_a\ Y_a\ Z_a]^T$

B. Proportional Deravitive Optimization for Posture Control

The optimization is done using the gradient of the effort function:

$$\nabla U = \left[\frac{dU}{dq_1}\ \frac{dU}{dq_2}\ \frac{dU}{dq_3}\ \frac{dU}{dq_4}\right] \tag{14}$$

Then a proportional derivative controller is used to calculate the posture torque (τ_p) as follows where K_p and K_d are tunable scalar PD gains:

$$\tau_p = -K_p \nabla U^T - K_d \dot{q} \tag{15}$$

The posture control torque would result in disturbing the task control unless isolation is made between the task space and the posture space. This is done by projecting the posture control in the null space of the task space as follows:

$$T_p = N^T \tau_p \tag{16}$$

where N^T is called the decoupling term for the PD controller:

$$N^T = I - J^T J^{-T} \tag{17}$$

V. Sliding Mode Controller

In this section the sliding mode controller on the 4-DOF INMOOV humanoid robot arm will be presented.

A. Sliding Mode Task Controller

A modification is done to add a sliding component element (μ_{sl}) to the task controller in equation (11) [20]:

$$f = \Lambda(q)f^* + \mu(q,\dot{q}) + p(q) + \Lambda(q)\mu_{sl} \tag{18}$$

The variable structure law is given by:

$$\mu_{sl} = -K_{sl}\frac{s}{\|s\| + \delta} \tag{19}$$

where the K_{sl} is a positive scalar constant acting as a gain and δ is a constant used to smooth the effect of the on-off controller that is harmful to the actuators.

The switching function (s) that follows insures that the error reaches zero is given by.

$$s = \dot{X}_e + K_s X_e \tag{20}$$

where K_s is a positive scalar constant, representing the slope of the sliding surface.

B. Sliding Mode Posture Controller

The posture control torque is then given as follows as in [20]:

$$\tau_{sp} = -K_{sp}\frac{M\hat{s}}{\|s\| + \delta_p} - MBR \tag{21}$$

where:

$$B = I - J^T(JJ^T)^{-1}J \tag{22}$$

$$R = -M^{-1}C - M^{-1}G \tag{23}$$

The estimated switching function ($\hat{s}$) of posture control:

$$\hat{s} = B\dot{q} + KB(\tfrac{dU}{dq})^T \tag{24}$$

The overall torque of the task and posture controller is as follows:

$$Total\ Torque = J^T f + N^T \tau_{sp} \tag{25}$$

The N^T term in eq. (25) insures that the posture space is in the null space of the task control. This term is important to emphasize that the posture control does not influence the task control.

$$N^T = I - J^T \Lambda J M^{-1} \tag{26}$$

VI. Simulation and Discussion

This section presents the simulation results of the proposed two controllers on the four degree of freedom INMOOV humanoid robotic arm, where the joints torques are limited to 3 Nm. due to the INMOOV servo motor specifications. Moreover, a comparison between the accuracy of the proportional derivative controller and the sliding mode controller are presented with the effort function gains tuned to the values shown in Table II.

TABLE II. Effort Function Gains

K_{a1}	K_{a2}	K_{a3}	K_{a4}
120	120	80	60
q_{L1}	q_{L2}	q_{L3}	q_{L4}
110°	170°	90°	-110°
K_{L1}	K_{L2}	K_{L3}	K_{L4}
1	1	1	1
δ_{L1}	δ_{L2}	δ_{L3}	δ_{L4}
0.1	0.1	0.1	0.1
K_L			
0.08			

© 2020 Int. J. Mech. Eng. Rob. Res

A. Proportional Derivative Controller

In this section the proportional derivative controller simulation results will be presented with the gains, after tuning, shown in Table III.

The simulation results of the PD controller provide satisfactory response and disturbance rejection as seen in the step response testing of the system in figures 3 to 5 with a relatively slow settling time in the x task variable and an overshoot in the z variable.

TABLE III. PD CONTROLLER PARAMETERS

K_x	K_v	K_p	K_d
220	20	10	5

Remark 1: the dotted lines in figures 3 to 5 represent the step response and the solid lines represent the step input. All these figures are in meters units.

The effort function can be seen in fig 6, that it was optimized by 38% from the peak effort. The joint angles to produce these step movements in x, y and z are shown in figure 7.

Remark 2: The effort function in figure 6 is dimensionless and the joint angles in figure 7 are in radians.

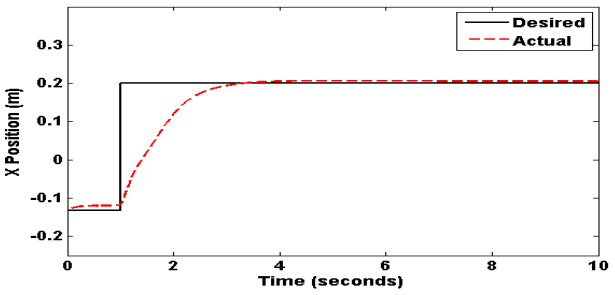

Figure 3. PD X-position

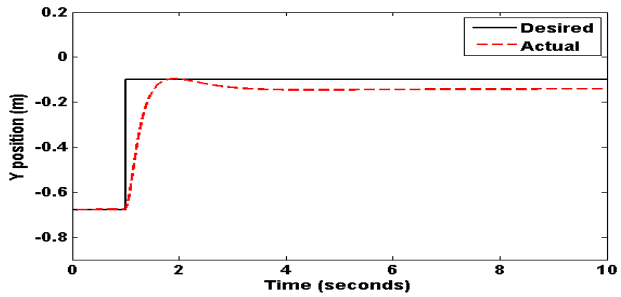

Figure 4. PD Y-position

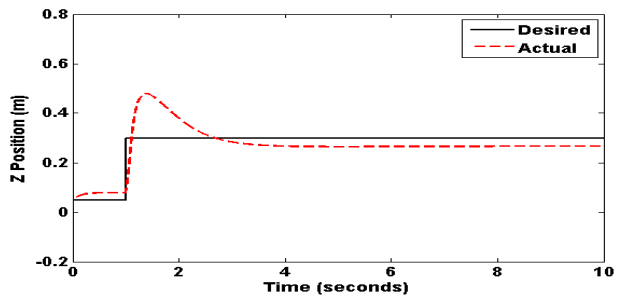

Figure 5. PD Z-position

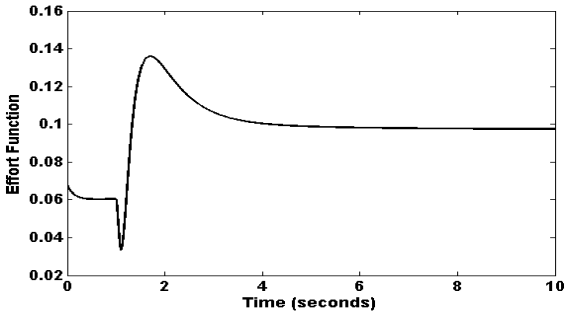

Figure 6. PD Effort Function

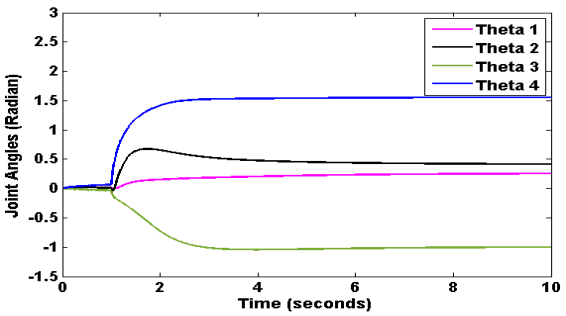

Figure 7. PD Joint Angles

B. Sliding Mode Controller

In this section the Sliding Mode Controller simulation results is presented with the gains in table 4. The simulation results of the SMC illustrate satisfactory settling time and disturbance rejection with no overshoot. The step response of the task variables of the SMC are shown in Figures 8 to 10. The small oscillations at the initial position, which is caused by the initial non-zero effort shown in figure 11.

The effort function optimization can be seen in figure 11 and the joint angles in figure 12.

Remark 3: the dotted lines in figures 8-10 represent the step response and the solid lines represent the step input. All these figures are in Meters.

Remark 4: the effort function in figure 11 is dimensionless and the joint angles in figure 12 are in radians.

TABLE IV. SMC PARAMETERS

K_x	K_v	K_{sl}	δ
5	4	250	0.3
K	K_{sp}	δ_p	K_s
100	1000	0.9	5

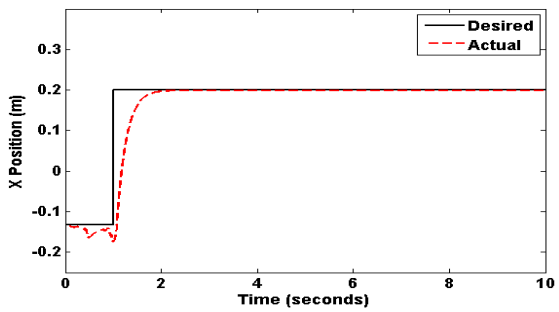

Figure 8. SMC X-position

© 2020 Int. J. Mech. Eng. Rob. Res

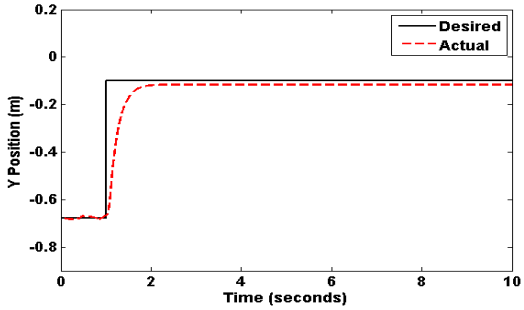

Figure 9. SMC Y-position

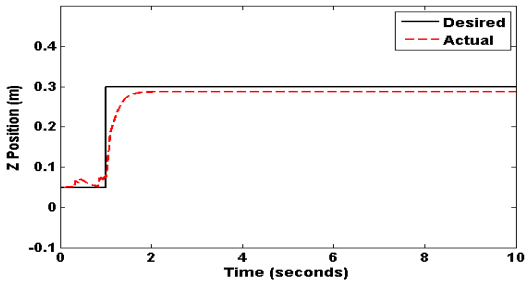

Figure 10. SMC Z-position

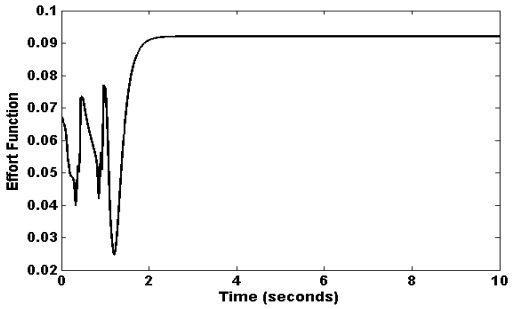

Figure 11. SMC Effort Function

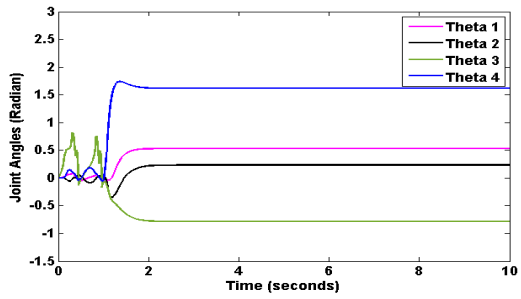

Figure 12. SMC Joint Angles

C. Comparison between PD and SMC

This section shows the comparison between SMC and PD control. As shown in Table V, the SMC is a great improvement from the PD control. The SMC has less settling time and less steady state error. The SMC is with an average of 22.7% better in root mean square error (RMSE) than the PD controller. Also, the SMC is better in decreasing the steady state error by an average of 68.4%, in decreasing the settling time by an average of 43.8% and in eliminating the overshoot completely.

The effort function comparison in Fig. 16 shows that the SMC decreased the effort by 8%.

Remark 5: the red lines in Figs. 13-16 are for the SMC and the blue lines are for the PD controller.

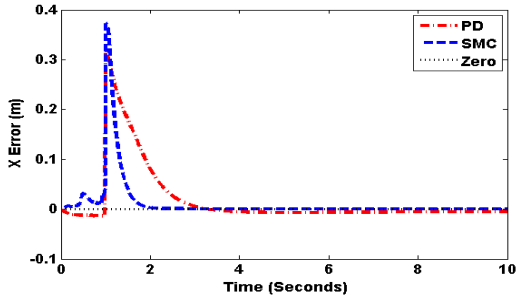

Figure 13. X-Error

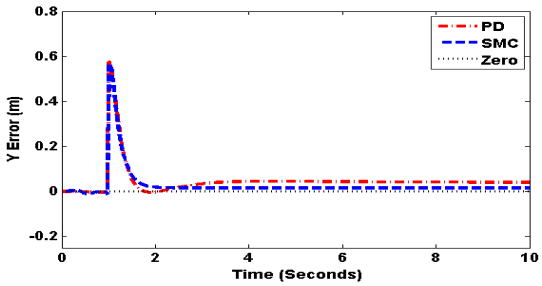

Figure 14. Y-Error

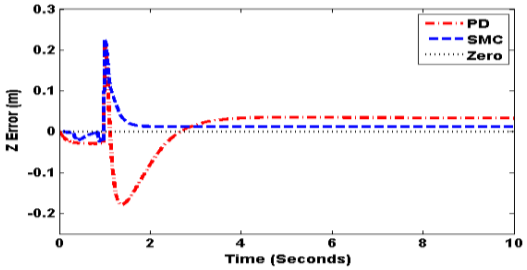

Figure 15. Z-Error

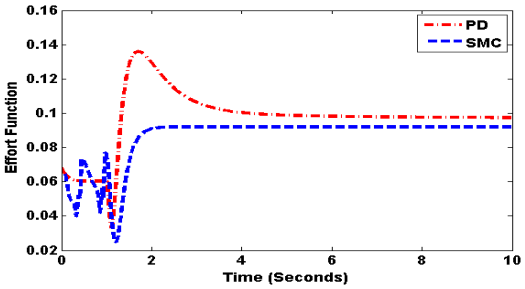

Figure 16. Effort Function

TABLE V. COMPARISON BETWEEN PD AND SMC

		PD	SMC	SMC ADVANTAGE
RMSE (m)	X	0.0632	0.0447	29.3%
	Y	0.0775	0.0812	-4.8%
	Z	0.0539	0.0303	43.8%
Steady State Error (m)	X	-0.0050	0.0009	82.0%
	Y	0.0408	0.0161	60.5%
	Z	0.0332	0.0124	62.7%
Settling Time (s)	X	3.0150	1.7330	42.5%
	Y	2.9650	1.8890	36.3%
	Z	3.056	1.4510	52.5%

© 2020 Int. J. Mech. Eng. Rob. Res

VII. Conclusion

This manuscript applies both proportional derivative and sliding mode controllers based on the operational space formulation of task/posture control on the open source INMOOV humanoid arm. Both controllers are simulated on MATLAB/Simulink using a Simscape multi-body model of the INMOOV arm. Based on studying the developed model, the results of comparison indicate that the SMC is better than the PD controller. As the sliding mode controller tracking RMSE error is an average 22.7% better than the PD controller. Moreover, the SMC shows its efficacy in decreasing the steady state error by an average of 68.4%, and in decreasing the settling time by an average of 43.8%. Furthermore, the effort function is used as an indicator of the natural movement of the arm which is also better in SMC. Simulation results show the effectiveness of the proposed sliding mode task/posture control on the INMOOV arm.

Acknowledgment

The authors wish to acknowledge the support of ASRT (Academy of Scientific Research & Technology in Egypt) for their endorsement of this research. Also, they would like to acknowledge the efforts of Gael Langevin on the open source INMOOV robot.

References

[1] S. Bruno and O. Khatib, eds. *Springer Handbook of Robotics*. Springer Science & Business Media, 2008.
[2] C. G. Atkeson et al., "Using humanoid robots to study human behavior," in *Proc. IEEE Intelligent Systems and their Applications*, vol. 15, no. 4, pp. 46-56, Jul/Aug 2000.
[3] Y. Kuroki, M. Fujita, T. Ishida, K. Nagasaka, and J. Yamaguchi, "A small biped entertainment robot exploring attractive applications," in *Proc.* 2003 IEEE International Conference on Robotics and Automation (Cat. No.03CH37422), 2003, pp. 471-476 vol.1.
[4] M. E. Rosheim, *Robot Evolution: The Development of Anthrobotics* (Wiley, New York 1994)
[5] M. Kim, S. Kang, S. Lee, W. Chung, K. Cho and Chong-Won Lee, "Development of a humanoid robot CENTAUR-design, human interface, planning and control of its upper-body," in *Proc. Conference 1999 IEEE International Conference on Systems, Man, and Cybernetics*, Tokyo, 1999, pp. 948-953 vol.4.
[6] A. Albers, S. Brudniok, J. Ottnad, C. Sauter, and K. Sedchaicharn, "Upper body of a new Humanoid Robot - the Design of ARMAR III," in *Proc. 2006 6th IEEE-RAS International Conference on Humanoid Robots*, Genova, 2006, pp. 308-313.
[7] F. Ni, C. Guo, Y. Liu, M. Jin, H. Liu, and Z. Zhang, "Design of an upper-body humanoid robot platform," in *Proc. 2017 IEEE International Conference on Mechatronics and Automation (ICMA)*, Takamatsu, 2017, pp. 1882-1887.
[8] Y. Dong, Z. Zhang, and H. Hu, "Development of an upper body humanoid robot," in *Proc. 2014 IEEE International Workshop on Advanced Robotics and its Social Impacts*, Evanston, IL, 2014, pp. 143-148.
[9] H. Cheng and G. Ji, "Design and implementation of a low cost 3D printed humanoid robotic platform," in *Proc.* 2016 IEEE International Conference on Cyber Technology in Automation, Control, and Intelligent Systems (CYBER), Chengdu, 2016, pp. 86-91.
[10] Spong, Mark W. Robot Modeling and Control. John Wiley & Sons, 2012.
[11] A. Aloulou and O. Boubaker, "On the dynamic modeling of an upper-body humanoid robot in the three-dimensional space," in *Proc. 10th International Multi-Conferences on Systems, Signals & Devices*, (SSD13), Hammamet, 2013, pp. 1-6.
[12] W. He, W. Ge, Y. Li, Y. J. Liu, C. Yang, and C. Sun, "Model identification and control design for a humanoid robot," in *Proc. IEEE Transactions on Systems, Man, and Cybernetics: Systems*, vol. 47, no. 1, pp. 45-57, Jan. 2017.
[13] S. A. Mohamed, S. A. Maged, and M. I. Awad, "Design and control of the lower part of humanoid biped robot," in *Proc. 2018 3rd International Conference on Robotics and Automation Engineering (ICRAE)*, Guangzhou, 2018, pp. 19-23.
[14] G. Simmons and Y. Demiris, "Imitation of human demonstration using a biologically inspired modular optimal control scheme," in *Proc. 4th IEEE/RAS International Conference on Humanoid Robots*, 2004., 2004, pp. 215-234 vol. 1.
[15] Spiers, Adam, et al. *Biologically Inspired Control of Humanoid Robot Arms: Robust and Adaptive Approaches*. Springer, 2016.
[16] O. Khatib, "A unified approach for motion and force control of robot manipulators: The operational space formulation," in *Proc. IEEE Journal on Robotics and Automation*, vol. 3, no. 1, pp. 43-53, February 1987.
[17] Slotine, E. Jean-Jacques, and L. Weiping, *Applied Nonlinear Control*, vol. 199, no. 1. Englewood Cliffs, NJ: Prentice hall, 1991.
[18] L. Qin, L. Liang, F. Liu, and Z. Jin, "The application of adaptive backstepping sliding mode for hybrid humanoid robot arm trajectory tracking control," in *Proc. the 2013 International Conference on Advanced Mechatronic Systems*, Luoyang, 2013, pp. 730-735.
[19] J. Y. Kuan and H. P. Huang, "Independent joint dynamic sliding mode control of a humanoid robot arm," in *Proc. 2008 IEEE International Conference on Robotics and Biomimetics*, Bangkok, 2009, pp. 602-607.
[20] A. Spiers, G. Herrmann, and C. Melhuish, "An optimal sliding mode controller applied to human motion synthesis with robotic implementation," in *Proc. the 2010 American Control Conference*, Baltimore, MD, 2010, pp. 991-996.

Omar T. Abdelaziz was born in Cairo, Egypt on 25 September 1995. Omar received his Bachelor in 2018 in Mechatronics from Ain-Shams University. Currently, he is studying MSc in Mechatronics in Ain Shams University. He is working as a teaching assistant in the Mechatronics Department in Ain Shams University. His research interests are humanoids, model predictive control, autonomous systems and robotics.

Shady A. Maged received his B.Sc. and M.Sc. degrees Mechatronics from the Ain-Shams University, Cairo, Egypt in 2010 and 2013 respectively. He worked as a Research and Lecturer Assistant in the University since 2010 till February 2014. In February 2014, he joined Egypt-Japan University for Science and Technology as a PhD student. He stayed in 2016 as a Visiting Researcher, in Namerikawa-Laboratory, Keio University. He received his PhD in Mechatronics and Robotics Engineering in 2017. In 2017 he joined the Mechatronics Engineering department Ain Shams University as an Assistant professor till now. His research interests are advanced model-based and intelligent control system, system dynamics, robotics, soft robotics and automation.

Mohammed Ibrahim Awad received his B.Sc and M.Sc. degrees in mechanical engineering from the Ain Shams University, Cairo, Egypt in 2001 and 2005 respectively, and the PhD degree in mechanical engineering from University of Leeds, Leeds, UK in 2012. He is currently working as an Associate Professor at Ain Shams University. His current research interests include mechatronic systems design, control and testing of lower limb prostheses, rehabilitation devices and robotics.

© 2020 Int. J. Mech. Eng. Rob. Res